Biointerface Research in Applied Chemistry
Open-Access Journal (ISSN: 2069-5837)

Article
Volume 13, Issue 5, 2023, 477
https://doi.org/10.33263/BRIAC135.477

Ultrastructural and Spectroscopic Analysis of Lignin of Stone Cells in *Mimusops elengi* L. (Sapotaceae) Fruit Mesocarp

Mamtaj Khatun [1,3], Kriti Ranjan Sahu [2,*], Amal Kumar Mondal [3,*]

1 Department of Botany, Egra S.S.B. College, Egra, Purba Medinipur, 721429, W.B., India; mamtajbotany@gmail.com (M.K.);
2 Department of Physics, Bhatter College, Datan, paschim Midnapore, 721426, W.B., India; kriti.basis2020@gmail.com (K.R.S.);
3 Department of Botany & Forestry Plant Taxonomy, Biosystematics & Molecular Taxonomy Laboratory Vidyasagar University, Midnapore-721102, West Bengal, India; amalcaebotvu@gmail.com(A.K.M.);
* Correspondence: amalcaebotvu@gmail.com (A.K.M.); kriti.basis2020@gmail.com (K.R.S);

Scopus Author ID 26025165000
Received: 26.09.2022; Accepted: 30.10.2022; Published: 3.01.2023

Abstract: Ultrastructural and spectroscopic analysis of lignin of stone cells of the fruit mesocarp of *Mimusops elengi* has been discussed here. Specific types of lignin, mostly present, Guaiacyj lignin (G-lignin), have been synthesized by Chemical methods and identified by Fourier Transform Infrared Spectroscopy (FTIR). An average domain (crystallite) size (L) of lignin is ~ 3.23 nm (32.3 Å) order calculated by X-Ray Diffraction (XRD). Calcium oxalate crystal (crystal sand type) has been seen in the sample and identified by the optical study by LM (Light microscopy), SEM (Scanning Electron Microscopy), Fluorescence Spectrophotometer, and FTIR. The essence of chemical compounds in our sample crystal and their structure has been determined by EDAX (Energy Dispersive X-ray Analysis) and XRD, respectively. The crystallite size of calcium oxalate is an average (187.5 ± 13.8) Å. Our present lignin is more active in the blue color region, analyzed by Chromatography plot using Fluorescence spectroscopy data under purple excitation light (380 nm). Also, we have studied the stone cells developed from parenchymal cells.

Keywords: *Mimusops elengi* fruit; XRD; FTIR; G-lignin; calcium oxalate; stone cell

1. Introduction

Mimusops elengi L. (Sapotaceae) tree is native to the Western peninsula. The Vernacular name of *Mimusops elengi* in English is Spanish cherry. Here, we have been focusing on *Mimusops elengi* fruit mesocarp grown in Purba Medinipur, Egra campus.

Fruit is an essential part of a plant. Spanish cherry fruit mesocarp contains stone cells. Brachysclereid is known as a stone cell, comprising a vast degree of lignin and cellulose, observed in the mesocarp layer, either aggregated or isolated forms known as sclereids [1,2]. Sclereids are developed from sclerenchyma cells—the secondary layout of lignin on the fundamental wall of parenchyma cells built sclereid [3,4]. Ca-base compounds, like Calcium Oxalate crystals in a different dimension, have been observed in different fruits.

The most abundant heterogeneous compound is lignin. It is a biopolymer in nature. It comprises up to one-third of plant cell walls [5]. Usually, it is evolved by the three

phenylpropane soloists, such as sinapyl alcohol, coniferyl alcohol, and p-coumaryl alcohol, through dehydrogenative polymerization. It is also linked through different types of Carbon-Carbon and ether bonds [6]. Three types of lignin units are present in nature, such as syringyl (S), guaiacyl (G), and p- hydroxyphenyl (H) types, as reported in the literature [7,8]. The chemical composition and structure of lignin [9] vary in different cells, cell layers, and plants. Hardwood lignin generally consists of G and S- type units, whereas softwood contains G-type units. In Gramineae (grasses, bamboo), three forms of lignin units (G, S, and H-types) exist, as reported in the literature [10,11]. Various preparation methods have classified lignin into milled wood lignin, acid-insoluble lignin, and alkali lignin [12]. Certain stains, like the Weisner reaction, have emerged as lignin's most widely used diagnostic tests. The $HOC_6H_3CH=CHCHO$ (coniferyl aldehyde) and $HO(CH_3O)_2C_6H_2CH=CHCHO$ (sinapyl aldehyde) groups of lignin appear to react with $C_6H_3(OH)_3$-HCl (phloroglucinol- HCl) to give a reddish-violet color. These reactive groups are only in small quantities in lignin, but the test is sensitive. This staining process is applied for identification and the appearance of lignin in the plant cell wall. Lignin is extensively distributed in plant cell walls and confers strength, rigidity, and impermeability. In several plants, it also gives both structural support and water transport. In terrestrial trees, 15-36% of dry wood consists of lignin. The 2nd most natural polymer in the universe is lignin. Lignin plays a significant role in cell wall thickening and stone cell creation [13,14].

CaC_2O_4 (Calcium oxalate) crystals were found in most edible plant tissues and organs reported by Webb in 1999 [15,16]. It was found in different morphological structures [17] like druses in *Pyrus malus* L. raphides in *Alocasia cucullata* Schott, styloids in *Tragia ramosa* Torr, prismatic in *Nymphaea tuberosa* Paine, and crystal sand in *Cordia subcordata* Lam.

Ultra-structure and spectroscopic analysis of *Mimusops elengi* L. (Sapotaceae) fruit mesocarp have been focused on in this research work. The identification and analysis have been made using different techniques such as Optical microscopic, Scanning Electron Microscopy (SEM), EDAX (Energy-dispersive X-ray spectroscopy), XRD (X-ray diffraction), FTIR (Fourier Transform Infrared), and fluorescence spectrophotometer.

2. Materials and Methods

2.1. Plant sample.

Living *Mimusops elengi* fruit collected from Egra S.S.B. college campus, used as a sample, has been exhibited in Figure 1.

Figure 1. (**a**) Tree of *Mimusops elengi*, (**b**) Fruit of *Mimusops elengi*, (**c**) Vertical cross section, and (**d**) Optical microscopic image (10x) of *Mimusops elengi* mesocarp.

2.2. Plant sample readiness for Light Microscopy (LM) and Auto Fluorescence (AF) in analysis.

The collected *Mimusops elengi* fruit were fixed in FAA (formalin: glacial acetic acid: 90% ethanol = 5:5:90) solution for preservation. The sample was dehydrated at 30℃ by 70, 85, 95, and 100 ethanol in percentage (30 min in each step) sequentially. The sample was cut into thin pieces with a thickness ~10 µm along the transverse section using a knife blade. 2-3 blobs of 1% $C_6H_3(OH)_3$- ethanol solution were poured on the surface of the cutting sample, placed on a glass plate, and after 2 to 3 minutes, 1 blob of 35% HCl was poured again on the same sample. The sample was covered by a glass coverslip for observation under FM (Fluorescence Microscope) with model no. LEICA DM 3000 and stone cell images were taken.

2.3. Stone cell preparation from the sample.

A warring blender is used to homogenize the ~ 5 g samples. 0.1 M NaCl is used to dilute the homogenized sample. The prolongation was trimmed for 30 min. at 22 ℃. Again the feces were trimmed for 30 min. with 500 ml of 0.5 N NaOH and decanted. Finally, the suspended sediment was kept in 500ml of 0.5 N HCl for 30 min., blended, and cleansed with water. This washing cleansing process was repeatedly done several times while the stone cells were free of extra cell debris. Stone cells were collected and then dried in the oven. The dried stone cells were weighed three times. 2.7% in wt stone cell (x) presents in our sample, and the used empirical Eq. (1) for calculation is

$$x(\%\ in\ wt.) = \frac{m}{M} \times 100 \quad \ldots \quad \ldots \quad \ldots \quad (1)$$

where M (in wt.) = used raw sample and m (in wt.) = collected dry stone cells.

2.4 . Lignin preparation from the sample

Chemical techniques have been used for lignin preparation [18]. Stone cells were well ground under 95% ethanol and ethanol: hexane (C_2H_5OH:C_6H_{14}) (1:2, v/v), dried, and repeated the process three times. Dried sediments were digested in 2 ml of 25% (v/v) C_2H_3Bro (acetyl bromide) in CH_3COOH (acetic acid) and incubated for 30 min at 70℃. The reaction was terminated by adding 0.9 ml of 2 N NaOH with an extra 5 ml of CH_3COOH and 0.1 ml of 7.5 M $HONH_2$.HCL (hydroxylamine hydrochloride). The lignin synthesis process is shown in Figure 2.

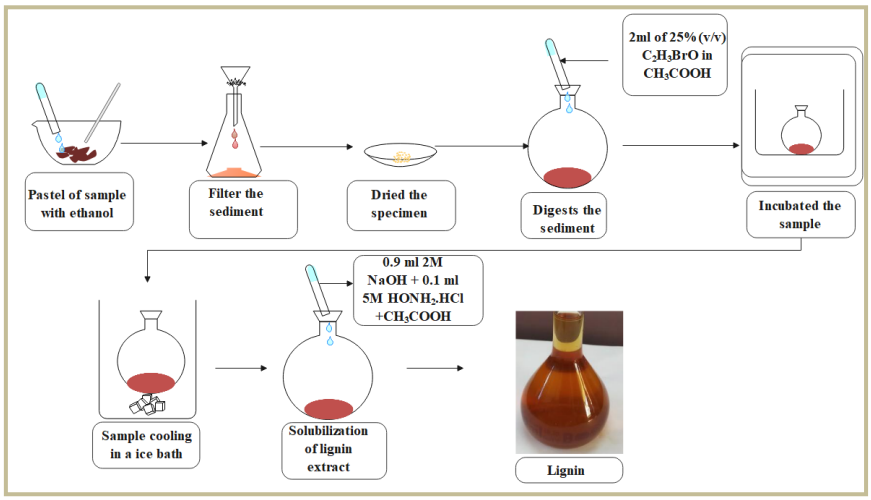

Figure 2. Schematic diagram of Lignin synthesis in the chemical process from *Mimusops elengi* fruit mesocarp.

2.5. Scanning Electron Microscopy (SEM).

The *Mimusops elengi* fruit tissue was cut with razor blades along a longitudinal section in 200 μm thickness. The cutting sample died under sunlight at room temperature and then coated with gold using a sputter coater. The final sample was viewed for Ultra-structural image and analysis. It has been taken out by scanning electron microscopy (SEM), ZEISS Supra-40 at IIT, Kharagpur, India.

2.6. Fourier Transform Infrared (FTIR) spectroscopy.

The *Mimusops elengi* fruit tissues were dried and ground by mortar and pestle for powder form. FTIR data were taken for analyzing the presence of functional groups in the samples, using Fourier Transform Infrared Spectroscopy, model no. JASCO FTIR 420 at Jadavpur University, Kolkata, India. FTIR data were taken in the band of 4000-400 cm^{-1}.

2.7. Fluorescence spectrophotometer.

FL characteristics analysis of lignin extracted from *Mimusops elengi* fruit tissues were prepared using chemical techniques described in detail in the previous sec. 2.4 and in Figure 2. The experiment was done by the Fluorescence spectrophotometer (HITACHI Model F-7000) with a slit width of 5 mm at Jadavpur University, Kolkata-32.

2.8. X-ray diffraction.

The Mesocarp of *Mimusops elengi* fruit tissue was dry at room temperature. The dry sample was grounded for 15 min by mortar and pestle and formed into a powder. The X-ray diffraction data of our powder sample was carried out at a scanning rate of 2º/min, with 2θ ranging from 1º to 50º, in a Bruker-ASX, Germany, diffractometer with Cu-kαl (= 1.5406 Å), kα2 (=1.54439 Å) and α-average filter radiation (λ = 1.5418 Å), operating at 30 kV and 10 mA. XRD data were analyzed using the software Origin 8.5.

3. Results and Discussion

3.1. Presence of lignin in stone cells.

We have cut the *Mimusops elengi* fruit in the longitudinal section for optical observation, characterization, and going through the Wiesner reaction [14]. Under the light microscope, the stone cell of *Mimusops elengi* are of different types, like spheroidal, and globoid [19], has been observed and shown in Figures 3a and 3b, and are viewed in reddish pink color. Due to the presence of lignin [20-22] in the stone cell. Orange color cells are the parenchyma cell indicated by orange arrows in Figure 3a and bounded by an orange color oval in Figure 3b. Stone cells are generated from parenchyma cells [14,23]. Figure 1c shows the Fluorescence images of the same stone cell in Figures 3a and 3b.

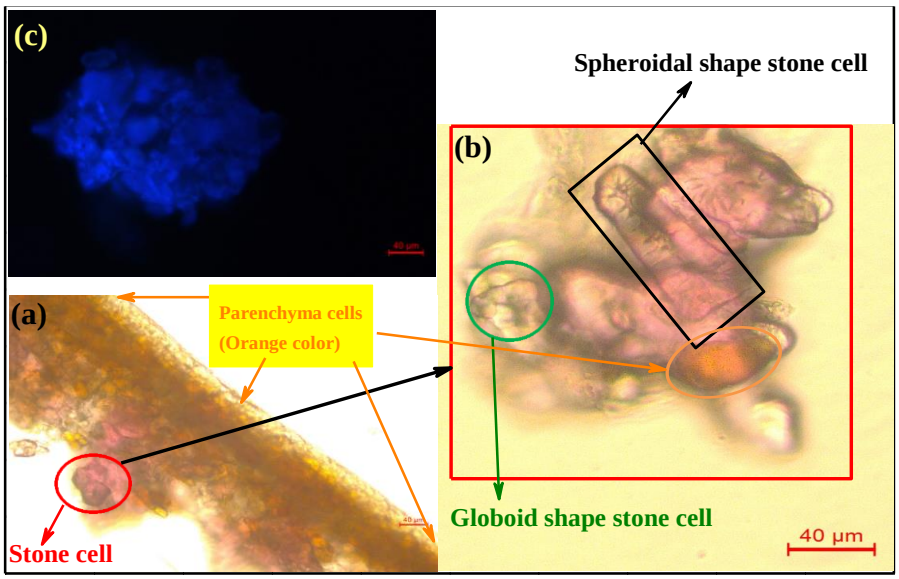

Figure 3. (a), (b) Sections stained with phloroglucinol-HCl; the lignin is present mainly in stone cells as a pink color. (**c**) Fluorescence images of stone cells.

3.2. SEM analysis.

Stone cells (SC), Cell Lumen (CL), Simple pits (SP), and Sclereid (SCL) were observed by SEM image, shown in Figures 4a & 4b. Secondary Cell Wall (SCW), Lamellar structure (LS), and Crystal Sand (CS) were observed in our SEM image in Figure 4c, and it indicates that the lignin cells were present.

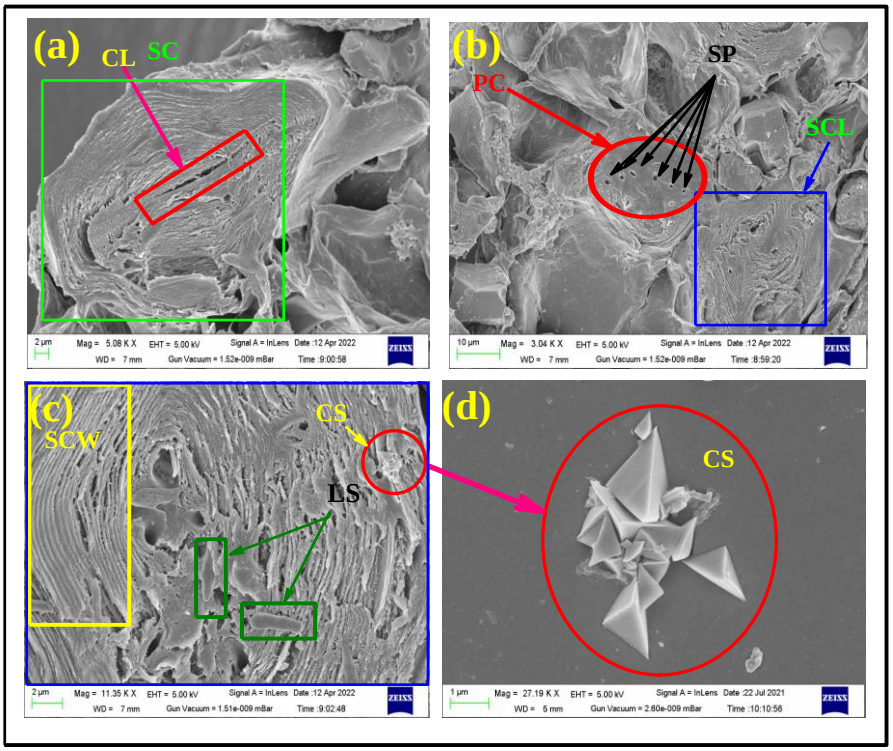

Figure 4. SEM micrographs of *Mimusops elengi* fruit epicarp show SC, CL, PC, SP, SCL, SCW, LS and CS. (**a**) Stone cell (SC), marked by green color rectangular boundary, Cell Lumen (CL), looks like canal type and marked by red color rectangular boundary, (**b**) Parenchyma cell (PC), marked by red color oval and looks like a solid surface. Some small holes were observed on the surface, and it was called Simple Pit (SP), Sclereid (SCL), marked by a blue color rectangular boundary (**c**) enlarging view of Figure 4b and specifically the SCL portion. The Secondary Cell Wall (SCW) looks like a ring layered type, marked by yellow color rectangular boundary, Lamellar structure (LS), marked by an olive color rectangular boundary, Crystal Sand (CS), marked by red color circular boundary, and (**d**) enlarging view of Figure 4c and specifically CS portion.

Stone cells show lamellar structure, expressing that the deposition of lignin in the cell wall formed the multi-layered and subsequently formed the distinct ring structure, as seen in the SEM photograph [14]. Crystal sand is present on the surface of the cell layer [24], shown in Figure 4c, and enlarging view in Figure 4d.

3.3. Lignin determination: the analysis of lignin functional groups of M. elengi.

3.3.1. `FTIR spectral characteristics.

FTIR spectroscopy is a powerful tool for the identification of organic compounds, the presence of chemical bonding as well as functional groups. FTIR data of lignin was recorded in Figure 5 and Table 2.

Table 1. FTIR absorption peaks and assignment of lignin extracted from the mesocarp of *Mimusops elengi*

Experimental Peak position (cm^{-1})	**Recommended Peak position (cm^{-1})**	**Assignments**	**Functional groups and structures in lignin/CaC_2O_4**	**Refs.**
512	515.23	O-C-O in-plane bending	CaC_2O_4	[25]
768	771.96	C=O asymmetrical stretching	CaC_2O_4	[26]
	750-860	C-H stretching	Aromatic ring (Lignin)	[32]
1027	1024.79	Aromatic C-H in-plane deformation (Lignin)	CaC_2O_4	[25,28]
	1030	C-O and C-H stretching	Aromatic ring and primary alcohol (Lignin)	[32]
1222	1215	C-O and C-C stretching	Ether (Lignin)	[32]
1313	1314	C–C symmetrical stretching	CaC_2O_4	[26,27]
	1316	C-O symmetric vibrating		
1366	1360-1370	C-H bending	$-CH_2$, $-CH_3$ (Lignin)	[31,32]
1440	1425-1460	C-H deformation	$-CH_2$, $-CH_3$ (Lignin)	[32]
1610	1615.25	C=O	CaC_2O_4	[25,40]
	1590-1610	C=O stretching	Aromatic skeletal vibrations plus (Lignin)	[31]
1731	1700-1750	C=O stretching	Unconjugated ketones, carbonyl, carboxyl, and aliphatic carbonyl (Lignin)	[32]
2070	2650-2890	C-H stretching	Methyl group in methoxyl (Lignin)	[32]
2921	2920	O-H stretching	Carboxylic hydroxyl (Lignin)	[32]
	2820-2960	C-H stretching	$-CH_2$, CH_3 (Lignin)	[32]
3292	3100-3400	O-H Stretching	Associated hydroxyl group (Lignin)	[32]

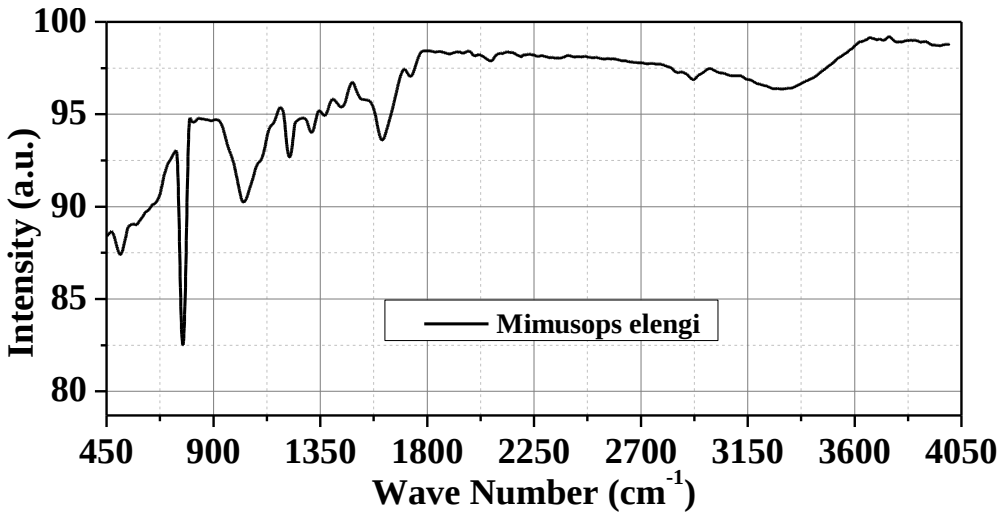

Figure 5. FTIR spectrum of lignin extracted from the fruit mesocarp of *Mimusops elengi*.

The observed FTIR absorption data in our experimental data strongly recommended for calcium oxalate (CaC_2O_4) compound, peaks at 512 cm^{-1}(for O-C-O in-plane bending), 768 cm^{-1} (for C=O asymmetrical stretching), 1027 cm^{-1} [25], 1113 cm^{-1} (C–C symmetrical stretching), and 1610 cm^{-1} (C=O) [25-27], and lignin for peaks at 768 cm^{-1} (C-H stretching), 1222 cm^{-1} (C-H stretching) [28], 1366 cm^{-1} (C-H bending) [29], 1440 cm^{-1} (C-H deformation), 1731 cm^{-1} (C=O stretching), 2070 cm^{-1} (C-H stretching), 2921 cm^{-1} (either O-H stretching or C-H stretching and or both) [30], 3292 cm^{-1} (O-H Stretching) [31,32]. Presents lignin in our sample is guaiacyl unit categories or G-type for peaks at 1222 cm^{-1} (C-O and C-C stretching), well matched with the reported data of [33]. (in detail discussed in Table 1).

3.3.2. Fluorescence spectrophotometer analysis.

Blue fluorescence of lignin in the stone cell was observed under purple excitation light (380 nm) [34]. Some authors reported [35-37] stone cells are abundant thick-walled tissue cells in pear fruit and are mainly composed of lignin. The cells of blue fluorescence were the stone cells. Scatterings of wavelengths in the visible electromagnetic spectrum can be quantified using CIE 1931 color coordinates, which are humans'physiologically apparent color. In this study, the emission spectra of *Mimusops elengi* were plotted using CIE 1931 Figure 6. The obtained color confirmed the different colors of emission of all materials. The color coordinate was (0.18219, 0.20313) [38,39] for *Mimusops elengi*. The non-emissive nature of *Mimusops elengi* was confirmed from the coordinates out of the CIE plot.

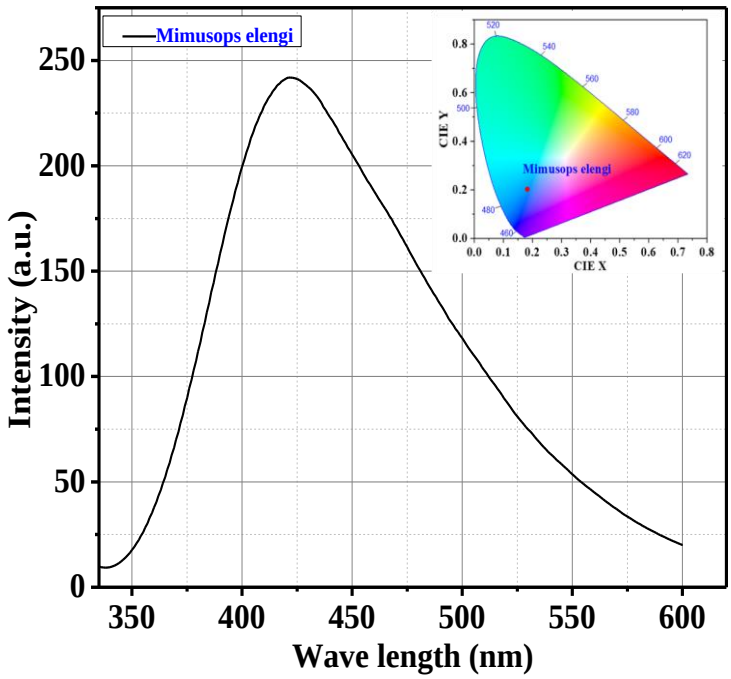

Figure 6. Fluorescence Spectrophotometer peak of lignin extract from *Mimusops elengi* fruit mesocarp, and CIE 1931 Chromaticity Diagram is in inset view

3.3.3. EDX analysis.

EDAX results, shown in Figure 7, give the Calcium (Ca) 8.91 wt% (3.41 in atomic %) and Carbon (C) 29.11 wt% (37.17 in atomic %) were present in our sample, and it was confirmed that crystal sand, has been shown in our SEM picture Figure 4, is Ca-base compound.

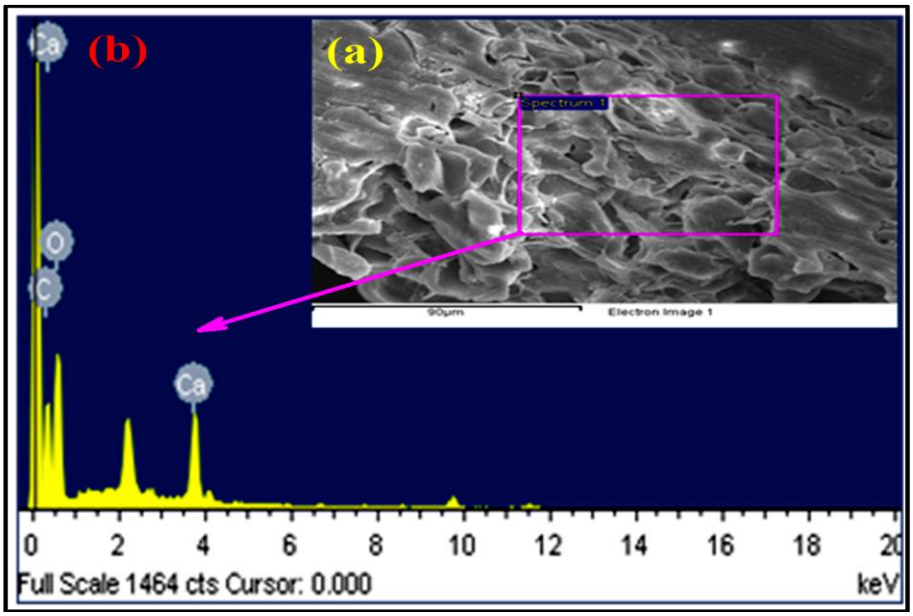

Figure 7. EDAX result of our sample. (**a**) SEM image, (**b**) Energy spectrum of the specified image, marked by a pink color rectangle.

3.3.4. XRD analysis.

XRD data gives the peaks at 14.99(101), 24.45(020), 30.16(220), and 38.24(130) for calcium oxalate [41]. A wide XRD peak in the range from 5° to 28° and a maxima peak at 21.98° has been observed. It indicates that the lignin is present [42-44], mostly G-type, confirmed by FTIR data and discussed ultra. An average domain (crystallite) size (L) of lignin is ~ 3.23 nm (32.3 Å) order, calculated using Scherre's equation, expressed in Eq. (2) [45,46]. An average crystallite size [47] of calcium oxalate is about ~ 18.74 nm (187.4 Å) (in details in Table 2).

$$L = \frac{0.94\lambda}{\beta cos\theta} \qquad (2)$$

Table 2. Crystal size of calcium oxalate for different planes and G-type lignin, observed in *Mimusops elengi*

Sample types	2 θ ˚	plane	β(FWHM in ˚)	L (Å)
Calcium oxalate	14.98	101	0.4362	191.9
Calcium oxalate	24.45	020	0.4541	187.0
Calcium oxalate	30.16	220	0.5070	169.6
Calcium oxalate	38.24	130	0.4367	201.2
Lignin	21.98	--	2.6023	32.5

L = Crystal size/domain order = 0.94λ/ βcosθ, λ = incident X-ray wavelength, β = FWHM (Full width at Half Maxima), θ = Bragg angle.

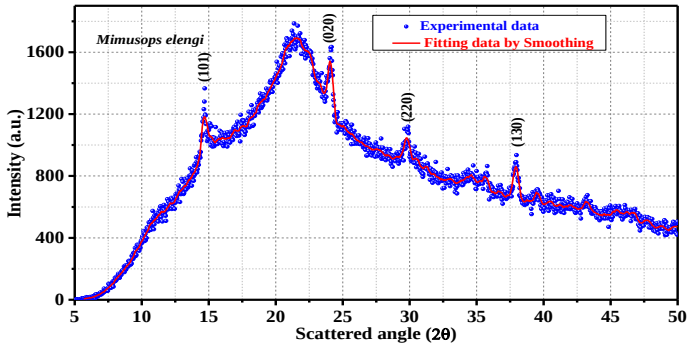

Figure 8. XRD data of *Mimusops elengi* fruit mesocarp. Blue solid points are the experimental data, and the continuous red line is the fitting data by smoothing (15 points) data.

4. Conclusions

The shape of the stone cell of *Mimusops elengi* fruit mesocarp is spheroidal and globoid, observed by Light microscopy. The stone cell is stained with phloroglucinol-HCL and shows-reddish-pink color. SEM study revealed that stone cells were observed in the form of aggregates surrounded by parenchyma cells in *M. elengi* fruit mesocarp. Stone cells show lamellar structure expressed that the deposition of lignin on cell wall formed multi-layered, forming the distinct ring structure, seen in SEM image.

Crystal sand is present on the surface of the cell layer. EDX analysis data inform us that the observed crystal is Ca base compound and a calcium oxalate type of crystal, confirmed by the presence of functional groups and supported by FTIR absorption peaks. XRD data gives the peak at 14.99° (101), 24.45° (020), 30.166° (220), and 38.24° (130) for calcium oxalate. The FTIR analysis data confirm that lignin functional groups are present in *M. elengi* fruit mesocarp, supported by the FTIR absorption peaks. Guaiacyl unit categories, i.e., G type lignin present in our sample and supported by the experimental FTIR peak, is 1222 cm^{-1}. The prominent XRD peak for lignin is 21.98°, and the average domain size is 32.5 Å. The synthesis lignin of our present work is observed by Fluorescence Spectrophotometer and is active in blue color under purple excitation light (380 nm.).

Funding

Self-funding.

Acknowledgments

The authors thank the USIC, Vidyasagar University, for providing facilities to study Fluorescence microscopy. The authors want to thank the CRF, IIT Kharagpur, for providing facilities to study SEM, XRD, and thanks to Egra S S B College, Egra, W.B., for providing the synthesis and optical Lab. The authors desire to express thanks to Jadavpur University for providing facilities to study FTIR, Fluorescence Spectrophotometer.

Conflicts of Interest

The authors have no conflict of interest.

References

1. Schroeder, C.A. Progress report on study of sclereid formation in avocado fruit pericarp.*California Avocado Society.***1982,***66*, 161-165, http://www.avocadosource.com/CAS_Yearbooks/CAS_66_1982/CAS_1982_PG_161-165.pdf.
2. Qiao, Y.J.; Zhang, S.L.; Tao, S.T.; Zhang, Z.M.; Liu, Z.L. Advances in research on developing mechanism of stone cells in pear fruit. *J. Fruit Science*. **2005**,*25*, 367-371,https://eurekamag.com/research/004/030/004030373.php.
3. Mamat, A.; Tusong, K.; Xu, J.; Yan, P.; Mei, C.; Wang, J. Integrated transcriptomic and proteomic analysis reveals the complex molecular mechanisms underlying stone cell formation in Korla pear. *Sci. Rep*. **2021,***11*, 7688,https://doi.org/10.1038/s41598-021-87262-3.
4. Antreich, S.J.; Xiao, N.; Huss, J.C.; Gierlinger, N. A belt for the cell: cellulosic wall thickenings and their role in morphogenesis of the 3D puzzle cells in walnut shell. *J. Experimental Botany*. **2022,***72*, 4744–4756,https://doi.org/10.1093/jxb/erab197.
5. Xiao, L.; Xu, F.; Sun, R-C. Chemical and Structural Characterization of Lignins Isolated from Caragana sinica. *Fibers and Polymers*. **2011**, *12*, 316-323,https://doi.org/10.1007/s12221-011-0316-9.

6. Mansouri, N.E.E.; Salvado, J. Structural characterization of technical lignins for the production of adhesives: Application to lignosulfonate, kraft, soda-anthraquinone, organosolv and ethanol process lignins. *Ind. Crops Prod*. **2006**, *24*, 8-16,https://doi.org/10.1016/j.indcrop.2005.10.002.
7. Ralph, J.; Lundquist, K.; Brunow, G.; Lu, F.; Kim, H.; Schatz, P.F.; Marita, J.M.; Hatfield, R.D.; Ralph, S.A.; Christensen, J.H.; Boerjan, W. Lignins: Natural polymers from oxidative coupling of 4-hydroxyphenylpropanoids. *Phytochem. Rev*.**2004,***3*, 29-60,https://doi.org/10.1023/B:PHYT.0000047809.65444.a4.
8. Zhang, J.; Cui, J.H.; Yin, T.; Sun, L.; Li, G. Activated effect of lignin on α-amylase. *Food Chem*. **2013,***141*, 2229-2237,https://doi.org/10.1016/j.foodchem.2013.05.047.
9. Yang, X.; Hou, S.; Chu, T.; Han, J.; Li, R.; Guo, Y.; Gong, Y.; Li, H.; Wan, Z. Preparation of magnesium, nitrogen-codoped carbon quantum dots from lignin with bright green fluorescence and sensitive pH response. *Industrial crops and products*. **2021**, *167*, 113507,https://doi.org/10.1016/j.indcrop.2021.113507.
10. Ross, K.; Mazza, G. Characteristics of lignin from flax shives as affected by extraction conditions, *Int. J. Mol. Sci.***2010**,*11*, 4035-4050,https://doi.org/10.3390/ijms11104035.
11. Maceda, A.; Rivera, J.R.; H., M.S.; Terazzas, T. Distribution and Chemical Composition of Lignin in Secondary Xylem of Cactaceae. *Chem. Biodiversity*. **2021**, *18*, e2100431,https://doi.org/10.1002/cbdv.202100431.
12. Yin, H.S.; Liu, H.M.; Liu, Y.L. Structural Characterization of Lignin in Fruits and Stalks of Chinese Quince. *Molecules*. **2017**,*22*, 890,https://doi.org/10.3390/molecules22060890.
13. Ranadive, A.S.; Haard, N.F. Peroxidase localization and lignin formation in developing pear fruit. *J. Food Sci.***1972**,*37*, 381-383,https://doi.org/10.1111/j.1365-2621.1972.tb02643.x.
14. Tao, S.; Khanizadeh, S.; Zhang, H.; Zhang, S. Anatomy, ultrastructure and lignin distribution of stone cells in two Pyrus species. *Plant Sci*. **2009,** *176*, 413–419,https://doi.org/10.1016/j.plantsci.2008.12.011.
15. Webb, M.A. Cell-mediated crystallization of calcium oxalate in plants. *Plant Cell.***1999,***11*, 751-761,https://doi.org/10.1105/tpc.11.4.751.
16. Vazquez, A.; Mendez, M. J.V.; Nicolas, B., J.; Chanona, P. J.J.; Fernandez, R.N.D.; Rivera, N.V.Effect of calcium oxalate crystals on the micromechanical properties of sclerenchyma tissue from the pecan nutshell (*Carya illinoinensis*).*Plant Physiology and Biochemistry*. **2022**, *170*,249–254,https://doi.org/10.1016/j.plaphy.2021.12.011.
17. Franceschi, V.R.; Horner, H.T.; Calcium oxalate Crystals in Plants. *The Botanical Review*.**1980**, *46*, 361-427,https://doi.org/10.1007/BF02860532.
18. Syros, T.; Yupsanis, T.; Zafiriadis, H.; Economous, A. Activity and isoforms of peroxidases, lignin and anatomy, during adventitious rooting in cuttings of *Ebenus cretica* L. *J. Plant Physiol*. **2004**,*161*, 69 – 77,https://doi.org/10.1078/0176-1617-00938.
19. Rao, T.A.; Bhupal, O.P. Typology of sclereids. *Proc. Indian Acad. Sci*.**1973**,*77*, 41–55,https://doi.org/10.1007/BF03045552.
20. Wang, H.; Feng, X.; Zhang, Y.; Wei, D.; Zhang, Y.; Jin, Q.; Cai, Y. PbUGT72AJ2-Mediated Glycosylation Plays an Important Role in Lignin Formation and Stone Cell Development in Pears (*Pyrus bretschneideri*). *Int. J. Mol. Sci*. **2022**, *23*, 7893,https://doi.org/10.3390/ijms23147893.
21. Xu, B.; Luis, L.; Trevino, E.; Sathitsuksanoh, N.; Shen, Z.; Shen, H.; Zhang, Y-H.P.; Dixon, R.A.; Zhao, B. Silencing of 4-coumarate:coenzyme A ligase in switchgrass leads to reduced lignin content and improved fermentable sugar yields for biofuel production. *New Phytologist*. **2011**,*192*, 611–625,https://doi.org/10.1111/j.1469-8137.2011.03830.x.
22. Xie, Z.; Rui, W.; Yuan, Y.; Song, X.; Liu, X.; Gong, X.; Bao, J.; Zhang, S.; Shahrokh, K.; Tao, S. Analysis of PRX Gene Family and Its Function on Cell Lignification in Pears (*Pyrus bretschneideri*). *Plants*. **2021**, *10*, 1874,https://doi.org/10.3390/plants10091874.
23. Wang, X.; Liu,S.; Sun, H.; Liu, C.; Li, X.; Liu, Y.; Lyu, D.; Du, G. Production of reactive oxygen species by PuRBOHF is critical for stone cell development in pear fruit. *Horticulture Research*. **2021**,*8*, 249,https://doi.org/10.1038/s41438-021-00674-0.
24. Franceschi, V. R.; Horner, H. T. Calcium Oxalate Crystals in Plants. *Botanical Review*. **1980**,*46*, 361–427,http://www.jstor.org/stable/4353973.
25. Vaitheeswari, S.; Sriram, R.; Brindha, P.; Kurian, G.A. Studying inhibition of calcium oxalate stone formation: an in vitro approach for screening hydrogen sulfide and its metabolites. *Int. Bra.z J. Urol*. **2015**, *4*, 503-510,https://doi.org/10.1590/S1677-5538.IBJU.2014.0193.

26. Karahaliloglu, Z.; Demirbilek, M.; Şam, M.; Saglam, N.; Denkbas, E.B. Surface-modified bacterial nanofibrillar PHB scaffolds for bladder tissue repair. *Artificial Cells, Nanomedicine, and Biotechnology*. **2016**, *44*, 74-82,https://doi.org/10.3109/21691401.2014.913053.
27. Nakata, P.A. Plant calcium oxalate crystal formation, function, and its impact on human health. *Front. Biol.* **2012,** *7*, 254–266,https://doi.org/10.1007/s11515-012-1224-0.
28. López,M. A.; Santiago, R.; Malvar, R.A.; Martín, D.; Pereira dos Santos, I.; Batista de Carvalho, L.A.E.; Faas, L.; Gómez, L.D.; da Costa, R.M.F. FTIR Screening to Elucidate Compositional Differences in Maize Recombinant Inbred Lines with Contrasting Saccharification Efficiency Yields. *Agronomy*.**2021**, *11*, 1130,https://doi.org/10.3390/agronomy11061130.
29. Intapun, J.; Rungruang, T.; Suchat, S.; Cherdchim, B.; Hiziroglu, S. The Characteristics of Natural Rubber Composites with Klason Lignin as a Green Reinforcing Filler: Thermal Stability, Mechanical and Dynamical Properties. *Polymers*. **2021,***13*, 1109,https://doi.org/10.3390/polym13071109.
30. Salim, R.M.; Asik, J.; Sarjadi, M.S. Chemical functional groups of extractives, cellulose and lignin extracted from native *Leucaena leucocephala* bar. *Wood science and Technology*. **2021**, *55*, 295–313,https://doi.org/10.1007/s00226-020-01258-2.
31. Ouyan, X.; Wang, W.; Yuan, Q.; Li, S.; Zhang, Q.; Zhao, P. Improvement of lignin yield and purity from corncob in the presence of steam explosion and liquid hot pressured alcohol. *RSC Advances*. **2015,** *5*, 61650-61656,https://doi.org/10.1039/C5RA12452B.
32. Sharma, S; Kumar, A. Lignin: Biosynthesis and Transformation for Industrial Applications, Springer Nature Switzerland AG, **2020**; 17-75,https://link.springer.com/book/10.1007/978-3-030-40663-9.
33. Li, J.; Li, B.; Zhang, X. Comparative studies of thermal degradation between larch lignin and manchurian ash lignin. *Polymer Degradation and Stability*. **2002,***78*, 279–285,https://doi.org/10.1016/S0141-3910(02)00172-6.
34. Xu, F.; Zhong, X.C.; Sun, R.C. Anatomy, ultrastructure and lignin distribution in cell wall of *Caragana korshinskii*. *Industrial crops and products.***2006**, *24*, 186-193,https://doi.org/10.1016/j.indcrop.2006.04.002.
35. Cai, Y.; Li, G.; Nie, J.; Li., Y.; Nie, F.; Zhang, J.; Xu, Y. Study of the structure and biosynthetic pathway of lignin in stone cells of pear. *Scientia Horticulturae*. **2010**, *125*, 374-379,https://doi.org/10.1016/j.scienta.2010.04.029.
36. Jin, Q.; Yan, C.; Qiu, J.; Zhang, N.; Lin, Y.; Cai, Y. Structural characterization and deposition of stone cell lignin in dangshan su pear. *Scientia Horticulturae*. **2013**, *155*, 123–130,https://doi.org/10.1016/j.scienta.2013.03.020.
37. Yan, C.; Yin, M.; Zhang, N.; Jin, Q.; Fang, Z.; Li, Y.; Cai, Y. stone cell distribution and lignin structure in various pear varities. *Scientia Horticulturae*. **2014**, *174*, 142-150,https://doi.org/10.1016/j.scienta.2014.05.018.
38. Elkhoshkhany, N.; Marzouk, S.; El–Sherbiny, M.; Anwer, H.; Alqahtani, M.S.; Algarni, H.; Reben, M.; Yousef, El.S. Investigation of structural and luminescence properties of borosilicate glass doped with Dy_2O_3. *Results in Physics*. **2021**, *27*, 104544,https://doi.org/10.1016/j.rinp.2021.104544.
39. Mirdda, J.N.; Mukhopadhyay, S.; Sahu K.R.; Goswami, M.N. Enhancement of optical properties and dielectric nature of Sm3+ doped Na_2O–ZnO–TeO_2 Glass materials. *J. Phys. Chem. Solids*. **2022**,*167*, 110776,https://doi.org/10.1016/j.jpcs.2022.110776.
40. Astete, R.J.; Davalos, J. J.; Zolla, G. Determination of hemicellulose, cellulose, holocellulose and lignin content using FTIR in *Calycophyllum spruceanum* (Benth.) K. Schum. and *Guazuma crinita* Lam.*PLOS ONE*. **2021,***16*, e0256559,https://doi.org/10.1371/journal.pone.0256559.
41. Šafranko, S.; Goman, S.; Goman, D.; Joki´c, S.; Marion, I.D.; Mlinari´c, N.M.; Selmani, A.; Medvidovi´c-Kosanovi´c, M.; Stankovi´c, A. Calcium Oxalate and Gallic Acid: Structural Characterization and Process Optimization toward Obtaining High Contents of Calcium Oxalate Monohydrate and Dihydrate. *Crystals*. **2021**, *11*, 954,https://doi.org/10.3390/cryst11080954.
42. Gupta, A.K.; Mohanty, S.; Nayak, S.K. Preparation and Characterization of Lignin Nanofibre by Electrospinnig Technique. *Int. J. Scientific Eng. Appl. Science*. **2015**, *3*, 184-191.
43. Goudarzi, A.; Lin, L.T.; Ko, F.K. X-Ray Diffraction Analysis of Kraft Lignins and Lignin-Derived Carbon Nanofibers. *J. Nanotechnol. Eng. Med.***2014**, *5*, 021006-1-021006-6,https://doi.org/10.1115/1.4028300.
44. El-Nemr, K.F.; Mohamed, H.R.; Ali, M.A.; Fathy, R.M.; Dhmees, A.S. Polyvinyl alcohol/gelatin irradiated blends filled by lignin as green filler for antimicrobial packaging materials. *Int. J. Environ. Analyt. Chem.***2020**, *100*, 1578-1602,https://doi.org/10.1080/03067319.2019.1657108.

45. Gomide, R.A.C.; De Oliveira, A.C.S.; Rodrigues, D.A.C.; De Oliveira, C.R.; De Assis, O.B.G.; Dias, M.V.; Borges, S.V. Development and Characterization of Lignin Microparticles for Physical and Antioxidant Enhancement of Biodegradable Polymers. *Polymers. J. Polym. Environ.* **2020**, *28*, 1326-1334,https://doi.org/10.1007/s10924-020-01685-z.
46. Sahu, K.R.; De, U.; Role of Nb_2O_5 phase in the formation of piezoelectric $PbNb_2O_6$. *Thermochimica acta*. **2014**,*589*, 25-30,https://doi.org/10.1016/j.tca.2014.05.008.
47. Paopun, Y.; Thanomchat, P.; Umrung, P.; Seraphin, S. Calcium Oxalate Crystals in Thai *Peperomia pellucida* (L.) Kunth Stems and Leaves. *Microsc. Microanal. Res*. **2022**,*35*, 26-32,https://ph02.tci-thaijo.org/index.php/mmres/article/view/246526.